Proc. Natl. Acad. Sci. USA
Vol. 96, pp. 3757–3762, March 1999
Cell Biology

Probing the *Saccharomyces cerevisiae* centromeric DNA (*CEN* DNA)–binding factor 3 (CBF3) kinetochore complex by using atomic force microscopy

LÍA I. PIETRASANTA*§, DOUGLAS THROWER†§¶, WAN HSIEH*, SHASHIREKHA RAO†, OLAF STEMMANN‡, JOHANNES LECHNER‡, JOHN CARBON†‖, AND HELEN HANSMA*‖

Departments of *Physics, and †Molecular, Cellular, and Developmental Biology, University of California, Santa Barbara, CA 93106; and ‡Institut für Biochemie, Genetik und Mikrobiologie, Universität Regensburg, 93040 Regensburg, Germany

Contributed by John A. Carbon, January 11, 1999

ABSTRACT **Yeast centromeric DNA (*CEN* DNA) binding factor 3 (CBF3) is a multisubunit protein complex that binds to the essential CDEIII element in *CEN* DNA. The four CBF3 proteins are required for accurate chromosome segregation and are considered to be core components of the yeast kinetochore. We have examined the structure of the CBF3–*CEN* DNA complex by atomic force microscopy. Assembly of CBF3–*CEN* DNA complexes was performed by combining purified CBF3 proteins with a DNA fragment that includes the *CEN* region from yeast chromosome III. Atomic force microscopy images showed DNA molecules with attached globular bodies. The contour length of the DNA containing the complex is ≈9% shorter than the DNA alone, suggesting some winding of DNA within the complex. The measured location of the single binding site indicates that the complex is located asymmetrically to the right of CDEIII extending away from CDEI and CDEII, which is consistent with previous data. The *CEN* DNA is bent ≈55° at the site of complex formation. A significant fraction of the complexes are linked in pairs, showing three to four DNA arms, with molecular volumes approximately three times the mean volumes of two-armed complexes. These multi-armed complexes indicate that CBF3 can bind two DNA molecules together *in vitro* and, thus, may be involved in holding together chromatid pairs during mitosis.**

Accurate chromosome segregation in mitosis and meiosis depends on the correct assembly of kinetochores on centromeric DNA (*CEN* DNA). During cell division, these structures attach chromosomes to the microtubules of the mitotic spindle and move the replicated chromosomes to opposing spindle poles.

The minimal functional centromere in the budding yeast *Saccharomyces cerevisiae* contains a 125-base-pair sequence (*CEN*) present once on each chromosome, which is organized into three domains: CDEI, CDEII, and CDEIII (Fig. 1*A*) (reviewed in ref. 1). CDEIII is an essential *CEN* DNA sequence element that provides the specific binding site for the multisubunit-protein-complex *CEN* DNA binding factor 3 (CBF3; ref. 2). The CBF3 complex consists of four proteins: Cbf3a (Cbf2p, Ndc10p, Ctf14p), Cbf3b (Cep3p), Cbf3c (Ctf13p), and Cbf3d (Skp1p). Mutations in the central CCG triplet of CDEIII, which inactivate the centromere *in vivo*, also interfere with CBF3–*CEN* DNA complex formation *in vitro* (2). Structures identifiable as kinetochores have not been imaged in yeast cells, nor have images previously been obtained of the CBF3–*CEN* DNA complex assembled *in vitro*.

In this paper, we describe the use of atomic force microscopy (AFM; also called scanning force microscopy) to probe the organization of the CBF3–*CEN* DNA complexes. We find that binding of the CBF3 proteins is associated with DNA shortening and bending. The location of the center of the CBF3 complex relative to the CDEIII site was found to be quite asymmetric, corroborating previous findings from DNase protection and DNA-protein crosslinking studies (2, 3). Additionally, we encountered evidence of joining or pairing of *CEN* DNA molecules by the CBF3 proteins. AFM has been successfully used to image biological samples in air or in liquid (4–8), and our findings further demonstrate that this imaging method is a powerful tool for the study of macromolecular assemblies and their interactions (9–16).

MATERIALS AND METHODS

Preparation of CBF3 Proteins. Cbf3a, Cbf3b, and Cbf3c/d complex proteins tagged with 6–10 histidine residues were overexpressed and purified from *Pichia pastoris*, *Escherichia coli,* and *S. cerevisiae,* respectively, according to the procedure described in ref. 23.

Preparation of *CEN* DNA Fragments and pUC19 DNA Beads. A linear DNA restriction fragment containing yeast centromere III was obtained from a *Nde*I-*Afl*III digest of pRN055 (17) and used for formation of the CBF3–*CEN* DNA complexes. This 914-bp DNA fragment has a single binding site for CBF3, and the central CCG triplet in CDEIII is located 489 bp (161 nm) from one end (Fig. 1*A*). For the control experiments, a mutated *CEN* DNA fragment containing a 3-bp deletion of the essential CCG was isolated from a *Nde*I-*Afl*III digest of pSF137 (a gift of Peter Sorger, Massachusetts Institute of Technology, Cambridge, MA). DNA fragments were incubated with the Klenow fragment of DNA polymerase I and dNTPs to convert overhanging single-stranded DNA to blunt ends. The restriction fragments were then purified by electrophoresis on 0.8% agarose gels and isolated by electroelution, extracted twice with phenol/chloroform, precipitated with ethanol, and redissolved in TE buffer (10 mM Tris-Cl, pH 8.0/1 mM EDTA). DNA samples were filtered through 0.025-μm Ultrafree-Probind membrane filters (Millipore) prior to use.

pUC19 DNA-coated beads were prepared by linearizing pUC19 with *Eco*RI, derivatizing the DNA by filling in the restriction end with biotin-14-dATP (Life Technologies), and

The publication costs of this article were defrayed in part by page charge payment. This article must therefore be hereby marked "*advertisement*" in accordance with 18 U.S.C. §1734 solely to indicate this fact.

PNAS is available online at www.pnas.org.

Abbreviations: *CEN* DNA, centromeric DNA; CBF3, centromere DNA binding factor 3; AFM, atomic force microscopy; FWHM, full width at half-maximum height.

§L.I.P. and D.T. contributed equally to this work.
¶Present address: Department of Biology, CB3280, University of North Carolina, Chapel Hill, NC 27599-3280.
‖To whom reprint requests should be addressed. e-mail: carbon@lifesci.lscf.ucsb.edu or hhansma@physics.ucsb.edu.

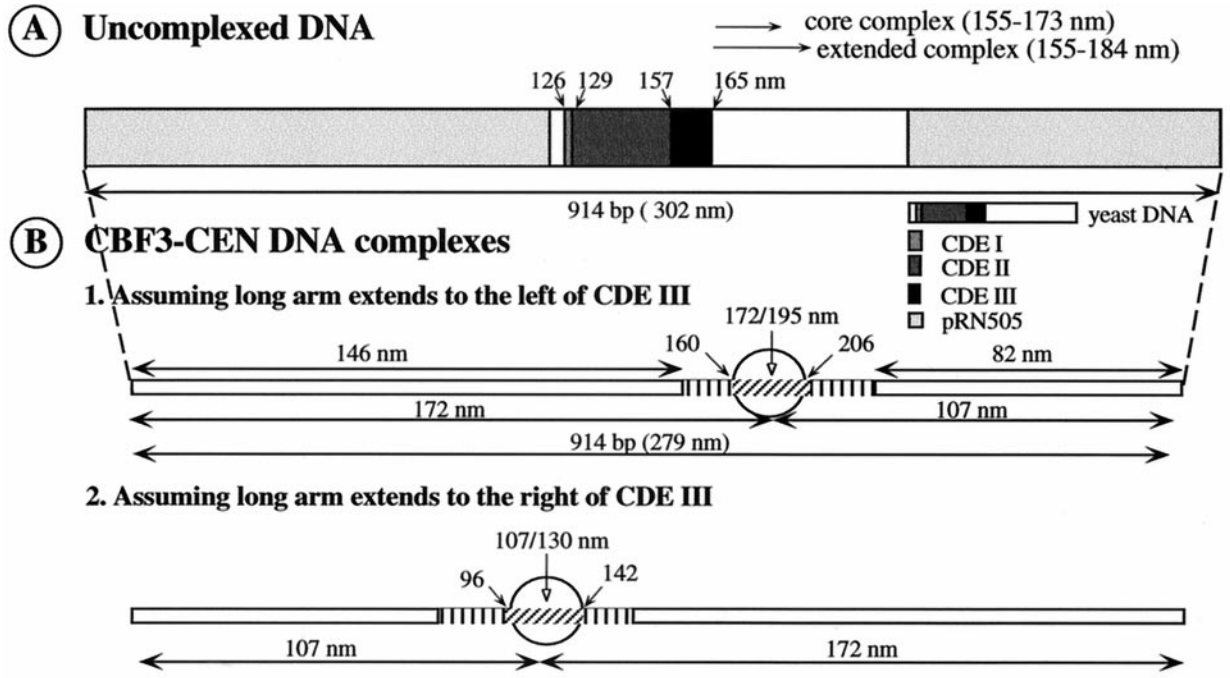

FIG. 1. Location of the CBF3 complex on yeast *CEN* DNA. (*A*) Scaled diagram of the linear 914-bp *CEN* DNA *Nde*I/*Afl*III restriction fragment showing the locations (in nanometers, numbered from the left) of CDEI, CDEII, and CDEIII. (*B*) Scaled diagrams illustrate this DNA molecule containing a CBF3 complex. The region of DNA covered by the CBF3 complex is indicated by a circle and the 23-nm reduction in contour length is indicated by a vertical arrow within the circle. The diameter of the circle shows the width of the complex at half-maximal height. The vertical stripes on each side of the circle indicate the apparent width of the base of the CBF3 complex, which is broadened by an amount comparable to the width of the AFM tip. In diagram B-1 the location of the complex relative to CDEI and CDEIII assumes that the long DNA arm extends to the left of CDEIII. In B-2, it is assumed that the long DNA arm extends to the right of CDEIII. All measurements are in nm. The core and extended complexes are indicated according to refs. 2 and 3.

incubating 400 μg of biotinylated DNA with 0.2 ml of streptavidin agarose beads (GIBCO/BRL).

Assembly of CBF3–*CEN* DNA Complexes for AFM Analysis. CBF3 proteins were added to a buffer containing 40 mM Na-Hepes, pH 7.6, 10 mM $MgCl_2$, 10% glycerol, 92 mM KCl, 16 mM NaCl, plus the appropriate *CEN* DNA fragment. Proteins were added to *CEN* DNA in a molar ratio (Cbf3a/b/c/d/DNA) of 3:3:1:1:1. This mixture was incubated for 20 min at room temperature in the presence of 10 μl of pelleted pUC19-coated agarose beads (as nonspecific DNA competitor). Following the incubation, an aliquot of the mixture was pipetted from the tube without disturbing the agarose beads that had settled to the bottom, then diluted 10-fold into 40 mM Na Hepes, pH 7.6, 10 mM $MgCl_2$, and 20-μl aliquots were immediately deposited on mica. After 2 min in a humidifying chamber, the mica disc was washed with 1 ml of MilliQ water (Millipore) and dried briefly in a stream of compressed and filtered air. All samples were further dried in a 2-liter glass dessicator in the presence of P_2O_5 for 5 min.

Sample Preparation for Proteins. A 20-μl drop of the solution containing the purified Cbf3a protein was pipetted onto freshly cleaved mica and rinsed with 1 ml of MilliQ water after 2 min. The Cbf3a was also spread on freshly cleaved mica by the action of the cationic detergent cetylpyridinium chloride as described previously (18).

E. coli RNA polymerase elongation complexes were formed with a 373-bp DNA template according to the procedure described in refs. 8 and 19.

AFM (Tapping Mode). In tapping-mode AFM, a tip on the end of an oscillating cantilever briefly touches the surface during each oscillation as it scans the sample. The cantilever is modulated sinusoidally at high frequencies. Its response is used as the input to a feedback loop, adjusting the piezo height such that the vibration amplitude stays constant. This mode is analogous to the constant deflection mode in conventional AFM. Tapping-mode AFM was performed in dry nitrogen using a Nanoscope III Multimode-AFM (Digital Instruments, Santa Barbara, CA) with an E-type vertical-engage piezoelectric scanner having a maximal lateral range of 12 μm. Standard silicon cantilevers 125 μm in length were used. Cantilever oscillation frequency was tuned to the resonance frequency of the cantilever (280–350 kHz). The 512 $\times$ 512 pixel images were captured with a scan size between 0.6 and 2 μm at a scan rate of 1 to 2 scan lines per sec. Images were acquired simultaneously with the height and the phase signals.

Images were processed by flattening using NANOSCOPE software (Digital Instruments) to remove background slope. Height, full width at half-maximum height (FWHM), and volume of the CBF3, and average height and width of the DNA molecules were measured with the NANOSCOPE software. In the analysis of cross-sections, the FWHM measurements were used as a first-order compensation for the systematic distortions introduced by the conical tip geometry (20). The contour length of DNA molecules was measured using NIH-IMAGE software v.1.59 (National Institutes of Health). Arm length percentages were calculated relative to the total length of DNA molecules within the same scan.

The DNA bending angles at the protein binding sites were measured with NIH-IMAGE software by drawing lines through the DNA axes on both sides of the protein and measuring the angle at their intersection (21). The DNA bending angle θ is then defined as $\theta = 180 - \alpha$. A second criteria was used to measure the bend angles in free DNA and CBF3–*CEN* DNA complexes. The orientational bias of the complex was evaluated by determining whether the angle formed between the DNA arms, when measured in a clockwise manner from the short to the long arm, was greater or less then 180°. Those that formed an angle less than 180° were classed as left-handed complexes and those that formed angles greater than 180° were classed as right-handed complexes (8).

The apparent molecular volumes of the protein complexes were measured by using the NANOSCOPE software in two ways. In using the bearing analysis software, the volumes of the molecules were measured from the top to the half-maximum height, and this value was doubled to obtain a corrected bearing volume. In a second method, after obtaining the height and FWHM, the molecular volume was calculated by treating the molecule as a segment of a sphere, as shown in Eq. **1** (22):

$$V_c = \pi(h/6)[3r^2 + h^2], \quad \textbf{[1]}$$

where V_c is the molecular volume, and h and r are the height and the radius of the protein, respectively. The radius r is half of FWHM.

In addition, the theoretical molecular volume was calculated from the protein's molecular weight, as shown in Eq. **2** (22):

$$V_{MW} = (M_0 N_0)(V_1 + dV_2), \quad \textbf{[2]}$$

where M_o is the molecular weight, N_o is Avogadro's number, V_1 and V_2 are the partial specific volumes of the individual protein (0.74 $cm^3 \cdot g^{-1}$) and water (1 $cm^3 \cdot g^{-1}$), respectively, and d is the extent of protein hydration (0.4 mol of H_2O per mol of protein).

Statistics. Data are given as mean values ± SEM. Significant differences in the results were evaluated by applying both Student's t test and the Wilcoxon test when applicable ($P < 0.05$). We have analyzed 40 uncomplexed DNA molecules and 94 CBF3–*CEN* DNA complexes.

RESULTS

AFM Imaging of CBF3 Complexes on Linear Fragments of *CEN DNA*. A linear 914-bp DNA restriction fragment containing a single copy of the centromere region of yeast chromosome 3 was combined with purified CBF3 proteins to form CBF3–*CEN* DNA complexes that could be analyzed by AFM (see *Materials and Methods*). The CDEIII element, which contains the DNA sequence that is most critical for CBF3 protein binding, is located near the center of the fragment (Fig. 1*A*). AFM images of these preparations revealed asymmetrically positioned conical structures that appeared to straddle a large proportion of the population of DNA molecules bound to the mica surface. Representative examples of these protein–DNA complexes are shown in Fig. 2. We identified these structures as CBF3 complexes because they were only observed in DNA samples that had been preincubated with a mixture of the four CBF3 subunit proteins. Protein–DNA complex formation required the addition of Cbf3a, Cbf3b, and Cbf3c/d, consistent with previous results from gel-mobility assays (23). Additionally, no complexes were found on *CEN* DNA fragments that lacked the central CCG of CDEIII, nor did these altered DNA fragments bind CBF3 in gel-mobility shift assays (ref. 24 and unpublished results).

The CBF3 protein complexes had outer diameters of 51 ± 1.7 nm (mean ± SEM, $n = 94$) and a FWHM of 21.8 ± 0.7 nm, as measured from AFM images. The measured heights of the complexes were 4.1 ± 0.1 nm.

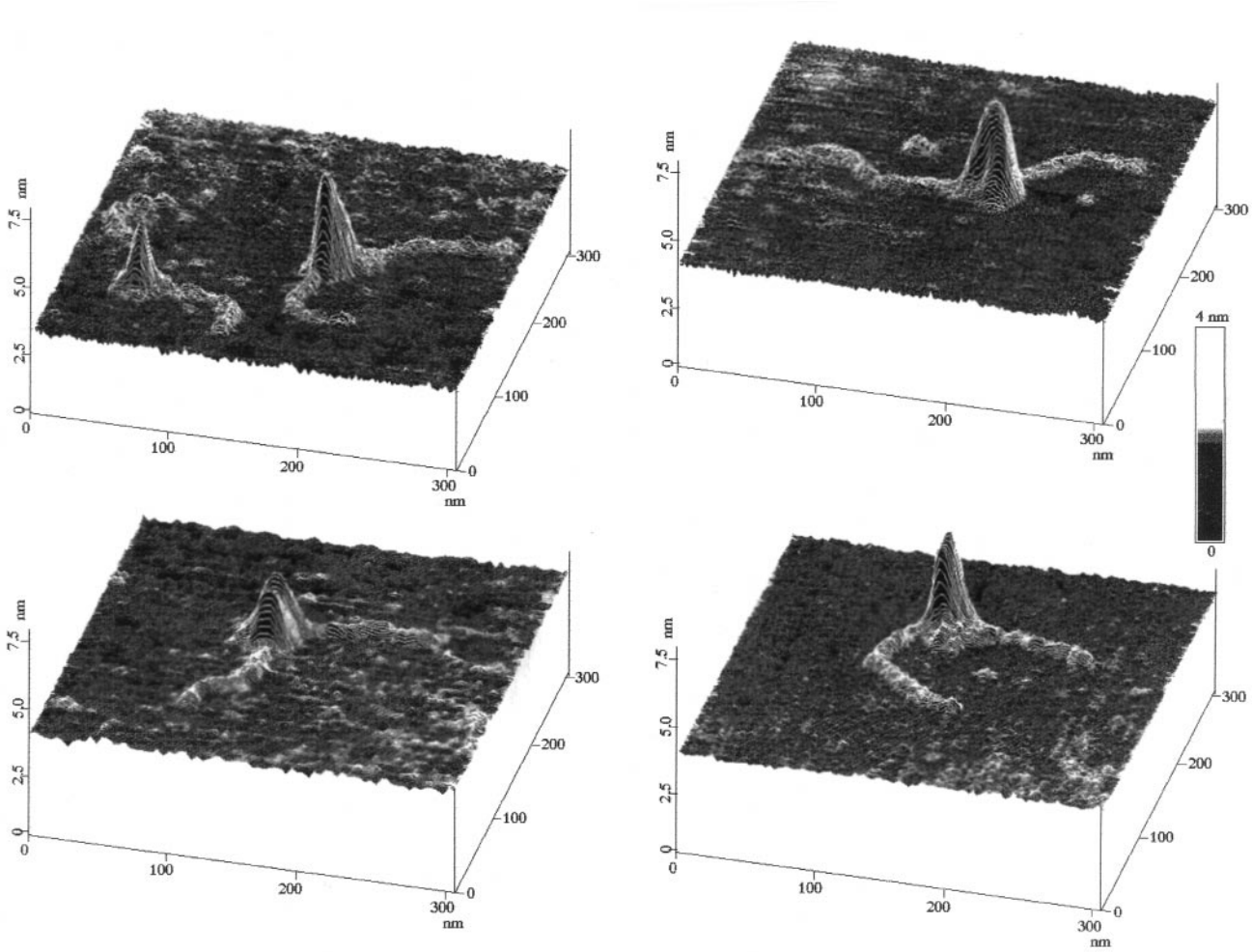

FIG. 2. AFM images of CBF3–*CEN* DNA complexes on mica. The images are presented as line plots at a 30° viewing angle to emphasize topography. Height is indicated by the gray-scale code bar.

Differences in Contour Lengths of DNA with and Without the CBF3 Complex. The apparent contour lengths of DNA molecules that lacked any visible bound proteins (free DNA) and those with bound proteins (complexed DNA) were measured from the AFM images. These measurements yielded normal distributions to which a Gaussian fit and a *t* test could be applied. The apparent contour length for the free DNA was 301.7 ± 2.0 nm. The measured length for the free DNA corresponded to a helical rise of 0.33 ± 0.01 nm/bp, which is in good agreement with the expected value of 0.34 nm/bp for B-DNA (25). The apparent contour length of complexed DNA molecules in the same sample was 23 nm less than that of free DNA (278.9 ± 2.6 nm). This difference was statistically significant, indicating that the binding of the CBF3 complex produces shortening of *CEN* DNA.

Location of the CBF3 Complex on *CEN* DNA. The location of the CBF3 complex relative to the DNA ends was determined by measuring the contour length of the two arms extended to either side of the complex. The contour lengths of the arms from the edge of the complex to the ends of the DNA molecule were 146 ± 2.3 nm and 81.6 ± 1.7 nm, respectively. These DNA arms represented 48% and 27%, respectively, of the length of the uncomplexed DNA molecule. Thus, the sum of both arms is 25% less than the contour length of the free DNA fragment (uncomplexed). This suggests the presence of a large region of contact between the proteins and the DNA molecules, although the actual dimensions of the protein–DNA complex are likely to be less than indicated by our results because of the presence of AFM tip-induced broadening effects (see *Discussion* and refs. 26 and 27). The outer diameter of the CBF3 complex (≈50 nm) is ≈17% of the length of the uncomplexed DNA. Measured from the geometric center of the complex, the protein was found to break the DNA into unequal arms of 171.8 ± 2.2 nm and 107 ± 1.7 nm. The center of the CDEIII region on this linear template is located 161 nm from one end of the uncomplexed DNA molecule. Thus, even accounting for the DNA shortening that occurs with the protein binding, the center of the protein complex does not coincide with the center of CDEIII (see *Discussion* and Fig. 1*B*).

DNA Bending and Conformation of the CBF3–*CEN* DNA Complexes. Images of CBF3–*CEN* DNA complexes revealed a distinct bend in the DNA molecules at the CBF3 binding site (Fig. 2). Measurements of the DNA bending angles yielded a broad distribution with an apparent bending angle of 55° ± 3.6° (Fig. 3). To determine if the bend was an inherent characteristic of this specific DNA molecule, representative molecules lacking complexes were examined for bending, using a mask centered at 171.8 nm from either end as the presumptive bend site. Uncomplexed DNA molecules showed a bend angle distribution centered at 0°, similar to results reported by other authors (14, 21). This suggests that the bending observed on the complexed DNA molecules was dependent on the binding of CBF3.

The bending angle and presence of two DNA arms of unequal length made it possible to determine if there was an orientational bias in the attachment of the CBF3–*CEN* DNA complex to the mica surface. Measuring angles in a counterclockwise direction starting from the short segment of the complexed DNA, we found that 39% of the complexes were right-handed versus 60% left-handed (see *Materials and Methods*). An equal distribution of right- and left-handed molecules would be expected if all sides of the complex bound with equal affinity to the surface. Our results indicate that no significant bias exists.

Molecular Volume of CBF3-DNA Complexes. The apparent molecular volume of the protein–DNA complex was measured from AFM images of CBF3–*CEN* DNA complexes. Measurements of 94 complexes by using the bearing volume analysis method (see *Materials and Methods*) yielded an average apparent molecular volume of 897 ± 47 nm^3. The average value for the molecular volume calculated from the height and width measurements of the complexes as applied to the formula for a segment of a sphere (see *Materials and Methods*) was 886 ± 68 nm^3. The distribution of measured volumes for the 94 complexes is shown in Fig. 4.

To determine whether this method generated reasonable protein volume measurements, we used purified Cfb3a protein and *E. coli* RNA polymerase. The result for the measured molecular volumes of the Cbf3a protein spread with or without detergent was 279 ± 35 nm^3 (bearing volume analysis method). The average values for the molecular volume calculated from the height and width measurements of the Cbf3a molecules as applied to the formula for a segment of a sphere (see *Materials and Methods*) were 224 ± 12 nm^3 in the absence of detergent and 219 ± 25 nm^3 in the presence of the detergent. For 53 complexes of RNA polymerase, we found a measured molecular volume of 882 ± 63 nm^3. The theoretical molecular volumes of monomeric Cbf3a and RNA polymerase calculated from their molecular weight, partial specific volume, and extent of hydration are 212 nm^3 and 851 nm^3, respectively (see *Materials and Methods*), in reasonably good agreement with the experimentally determined values.

Multi-Armed CBF3–*CEN* DNA Complexes. Approximately 12% of the protein–DNA complexes observed in our preparations contained more than two DNA arms (Fig. 5). Approximately equal numbers of three- and four-armed complexes

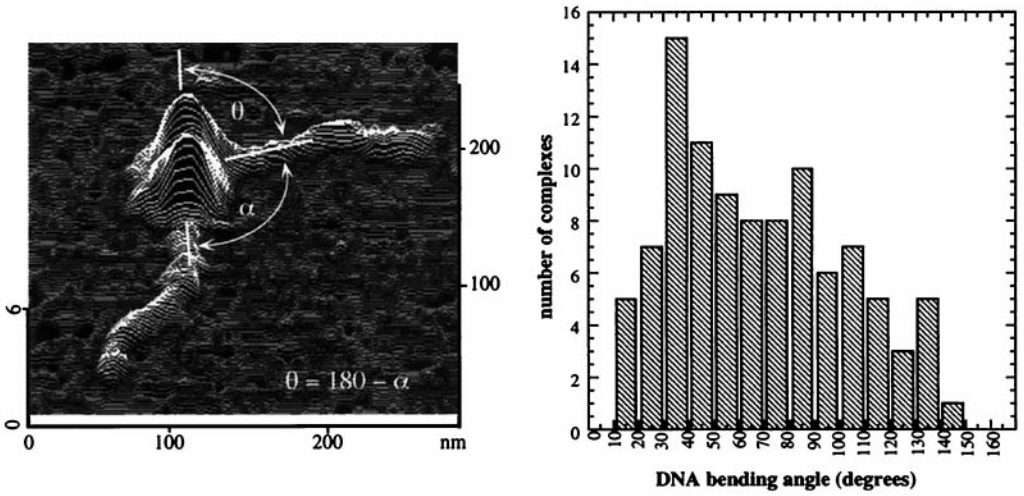

FIG. 3. *CEN* DNA is bent at the site of CBF3 binding. (*Left*) A typical CBF3–*CEN* DNA complex showing the measured angle α and its relation to the bend angle θ. (*Right*) Histogram of the DNA bend angles measured from AFM images of 94 CBF3–*CEN* DNA complexes.

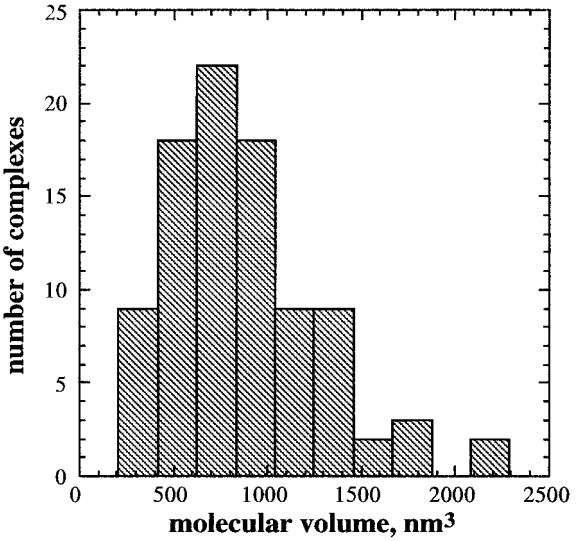

FIG. 4. Molecular volumes of CBF3–*CEN* DNA complexes. Histogram of the calculated volumes of the CBF3–*CEN* DNA complexes using the bearing volume method to analyze the AFM images (see *Materials and Methods*).

were observed. Two short and two long arms were observed in the four-armed complexes, indicating that they are formed by the fusion of the protein masses of a pair of two-armed complexes.

The apparent height for these complexes is 7.3 ± 0.4 nm, the width at half height is 28.7 ± 1.1 nm, and the measured volume is 2600 ± 288 nm^3. Thus, the average height is nearly twice the height of two-armed complexes, the width at half height is slightly greater than that of two-armed complexes, and the average volume is about three times the average measured volume for two-armed complexes.

DISCUSSION

Visualization of individual biological molecules by AFM has been used successfully to reveal details of protein–protein and protein–DNA interactions in a number of systems (4–7, 28). We have examined the interaction between the yeast CBF3 multisubunit protein complex and *CEN* DNA to directly answer questions relating to the conformation of DNA in the CBF3-bound state, and to determine the dimensions and volume of the protein complex. Volume measurements can be used to calculate the molecular mass of the complex and the most likely subunit stoichiometries.

The outer diameter of proteins and the width of DNA measured from AFM images is broadened by an amount comparable to the width and shape of the microtip used to image them (26, 27). The width of the probing tip can be estimated from width measurements of DNA molecules in the AFM images. We measured the width of 40 DNA molecules in our samples and obtained a mean value of 10.3 ± 0.3 nm. The diameter of double-stranded DNA obtained from x-ray crystallography data is 2.4 nm (25). Thus, it was estimated that tip broadening would contribute at least 8 nm to the apparent width of the CBF3 complex on the DNA. Additionally, the observed height of the DNA was 0.5 ± 0.01 nm, indicating that the tip compresses the DNA, as has been observed previously when AFM was used to image DNA molecules. To correct for tip-induced errors when calculating protein volumes, FWHM measurements have been used instead of full width (22). Thus, the FWHM measurement for CBF3 (21.8 nm) is probably a reasonable estimate of its actual diameter.

We determined that binding of the CBF3 complex to *CEN* DNA resulted in a statistically significant 23-nm reduction of the length of linear DNA fragments. This is equivalent to ≈70 bp of DNA. Other examples of protein-induced shortening of DNA have been reported and are thought to involve a nucleosome-like wrapping of the DNA around a protein core (29, 30). Making the assumption that the diameter of the complex is approximately 22 nm, the length of DNA that would be required to wrap once around the entire complex would be 69 nm, which is significantly greater than the observed CBF3-induced DNA shortening (23 nm). Thus, it is unlikely that the *CEN* DNA wraps around the entire CBF3 complex; possibly, the DNA loops or bends among a subset of proteins in the complex. A 23-nm loop of DNA would have *ca.* 70 bp. This is similar to the number of base pairs of *CEN* DNA (56–80 bp) that appear to interact with CBF3, based on DNase footprinting (2) and DNA–protein-crosslinking studies (3).

Our results show that the binding of CBF3 is not symmetrical with respect to CDEIII because the contact region extends primarily to the right of CDEIII, on the CDEII-distal side (see Fig. 1*A*). From contour-length measurements and the known nucleotide sequence, the CDEIII site on the 914-bp *CEN* DNA fragments lacking complexes would be located between 157 and 165 nm from one end. The center of the bound CBF3 complex divides the fragment into arms of 172 and 107 nm (the total length is 23 nm shorter than the uncomplexed DNA molecule, as explained above). Because we do not have a marker that independently distinguishes the two ends of the DNA fragments, there are two possible locations for the complex in relation to the position of CDEIII. The model shown in Fig. 1*B*-1 assumes that the long DNA arm extends to the left of CDEIII (the CDEI side). The DNA region shortened by 23 nm is assumed to be at the center of the complex (see vertical arrow, Fig. 1*B*), placing the borders of the shortened region between 172 and 195 nm. A 22-nm-diameter complex would then extend between 160 and 206 nm, overlapping and extending well to right of CDEIII. The alternative scenario that the long DNA arm extends to the right of CDEIII (Fig. 1*B*-2) would place the center of the complex to the left of CDEI, with the complex extending into CDEII, but not including CDEIII. The interpretation shown in Fig. 1*B*-1 is by far the most likely because it is consistent with the results of DNase protection and crosslinking studies (2, 3).

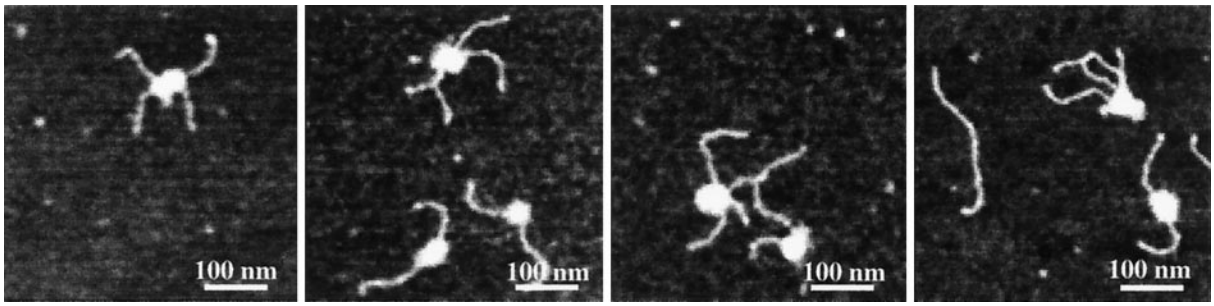

FIG. 5. Multi-armed CBF3–*CEN* DNA complexes. AFM images (top views) of complexes containing single and multiple DNA molecules. (Image sizes are 500 × 500 nm.)

We also observed that *CEN* DNA bending was associated with the binding of CBF3. Evidence for such an interaction between CBF3 and *CEN* DNA had not previously been found. Protein-induced DNA bending is involved in a variety of functions including transcriptional regulation by upstream trans-acting factors (31), DNA repair (13), the action of endonucleases (32), and maintenance of higher order chromatin structure (33). CBF3-induced DNA bending might facilitate interactions between CBF3 proteins and other centromere proteins, such as Cbf1p and Cse4p, that have been shown to interact genetically with CBF3 (34). It has been speculated that Cse4p, a protein with sequence homology to *CEN*P-A and histone H3, may be involved in the folding of *CEN* DNA into a nucleosome-like structure (35). Future AFM experiments on *CEN* DNA complexes containing CBF3, Mif2p, Cse4p, and a full histone complement could help determine if such a model is correct.

Efforts to determine the molecular mass of the CBF3 complex have been hindered by the fact that the formation of this complex requires binding of the proteins to DNA (23). With AFM, the molecular mass of the CBF3 complex can be estimated from its measured molecular volume. The molecular mass can be estimated by using a published standard curve that has the molecular volumes from AFM of proteins with known molecular masses (22). Using this method with our molecular volumes for *E. coli* RNA polymerase, we estimate a molecular mass of ≈480 kDa, which is in good agreement with the known value of ≈450 kDa (36).

For the Cbf3a protein, we obtained an estimated molecular mass of ≈120 kDa, which is close to the predicted molecular mass of 110 kDa (37, 38). Although the Cbf3a protein exists in solution as a multimer (23), apparently it binds to the mica surface as a monomer in the presence of detergent or at low ionic strength.

For the CBF3 protein complex, the apparent molecular mass was ≈480 kDa. This exceeds the size expected for a complex composed of four monomers and is similar to the hypothetical molecular mass of the CBF3 core complex as modeled by Espelin *et al.* (3), containing two molecules of Cbf3a, two Cbf3b, one Cbf3c, and one Cbf3d (total of 430 kDa). Only a single size population was apparent from our volume-distribution results (Fig. 4), but the wide range of this distribution could indicate the presence of complexes with a variety of subunit stoichiometries.

A significant number (12%) of the CBF3–*CEN* DNA complexes had either three or four DNA arms (Fig. 5), suggesting that dimerization of the DNA was occurring. The CBF3 protein complexes on these three- and four-armed structures were also two to three times as large as the CBF3 complexes on two-armed structures. Naked DNA molecules in preparations lacking CBF3 proteins did not interact with the frequency with which the multi-armed complexes were observed, suggesting that the interaction was mediated by interactions between CBF3 proteins bound to centromeres on two DNA molecules. We assume in the case of the three-armed complexes that one arm is not visible because it is under the complex. It is possible that these multi-armed complexes could be responsible, at least in part, for the lower mobility bands that have been observed in gel-shift assays with CBF3 and *CEN* DNA (2, 3, 24, 39). Alternatively, these dimer molecules could be too large to penetrate polyacrylamide gels or too unstable to survive gel electrophoresis. Thus they would not be detected in standard DNA-fragment mobility-shift experiments. It is tempting to speculate that CBF3 proteins could be involved in sister chromatid cohesion, although no *in vivo* evidence currently supports a direct role of these proteins in this process.

The authors thank Roxana Golan, Xomalin Peralta, and Claire Wyman for discussions that were extremely helpful. This research was supported by grants from the National Cancer Institute, National Institutes of Health (CA-11034 to J.C.), and National Science Foundation (MCB 9604566 to H.H.). O.S. and J.L. were supported by a grant from the Deutsche Forschungsgemeinschaft. J.C. is an American Cancer Society Research Professor.

1. Lechner, J. & Ortiz, J. (1996) *FEBS Lett.* **389,** 70–74.
2. Lechner, J. & Carbon, J. (1991) *Cell* **64,** 717–725.
3. Espelin, C. W., Kaplan, K. B. & Sorger, P. K. (1997) *J. Cell Biol.* **139,** 1383–1396.
4. Bustamante, C. & Rivetti, C. (1996) *Annu. Rev. Biophys. Biomol. Struct.* **25,** 395–429.
5. Bustamante, C., Rivetti, C. & Keller, D. J. (1997) *Curr. Opin. Struct. Biol.* **7,** 709–716.
6. Colton, R. J., Baselt, D. R., Dufrêne, Y. F., Green, J. B. & Lee, G. U. (1997) *Curr. Opin. Chem. Biol.* **1,** 370–377.
7. Czajkowsky, D. M. & Shao, Z. (1998) *FEBS Lett.* **430,** 51–54.
8. Hansma, H. G., Bezanilla, M., Nudler, E., Hansma, P. K., Hoh, J., Kashlev, M., Firouz, N. & Smith, B. L. (1998) *Probe Microscopy* **1,** 127–134.
9. Erie, D. A., Yang, G., Schulz, H. C. & Bustamante, C. (1994) *Science* **266,** 1562–1566.
10. Pietrasanta, L. I., Schaper, A. & Jovin, T. M. (1994) *Nucleic Acids Res.* **22,** 3288–3292.
11. Wyman, C., Grotkopp, E., Bustamante, C. & Nelson, H. C. M. (1995) *EMBO J.* **14,** 117–123.
12. Allison, D. P., Kerper, P. S., Doktycz, M. J., Thundat, T., Modrich, P., Larimer, F. W., Johnson, D. K., Hoyt, P. R., Mucenski, M. L. & Warmack, R. J. (1997) *Genomics* **41,** 379–384.
13. Cary, R. B., Peterson, S. R., Wang, J., Bear, D. G., Bradbury, E. M. & Chen, D. J. (1997) *Proc. Natl. Acad. Sci. USA* **94,** 4267–4272.
14. Rippe, K., Guthold, M., von Hippel, P. H. & Bustamante, C. (1997) *J. Mol. Biol.* **1997,** 125–138.
15. Yaneva, M., Kowalewski, T. & Lieber, M. R. (1997) *EMBO J.* **16,** 5098–5112.
16. Wyman, C., Rombel, I., North, A. K., Bustamante, C. & Kustu, S. (1997) *Science* **275,** 1658–1661.
17. Ng, R. & Carbon, J. (1987) *Mol. Cell. Biol.* **7,** 4522–4534.
18. Schaper, A., Starink, J. P. P. & Jovin, T. M. (1994) *FEBS Lett.* **355,** 91–95.
19. Bezanilla, M., Drake, B., Nudler, E., Kashlev, M., Hansma, P. K. & Hansma, H. G. (1994) *Biophys. J.* **67,** 2454–2459.
20. Fritzsche, W., Schaper, A. & Jovin, T. M. (1994) *Chromosoma* **103,** 231–236.
21. Rees, W. A., Keller, R. W., Vesenka, J. P., Yang, G. & Bustamante, C. (1993) *Science* **260,** 1646–1649.
22. Schneider, S. W., Lärmer, J., Henderson, R. M. & Oberleithner, H. (1998) *Pflügers Arch.* **435,** 362–367.
23. Stemmann, O. & Lechner, J. (1996) *EMBO J.* **15,** 3611–3620.
24. Sorger, P. K., Doheny, K. F., Hieter, P., M., K. K., Huffaker, T. C. & Hyman, A. A. (1995) *Proc. Natl. Acad. Sci. USA* **92,** 12026–12030.
25. Wing, R. M., Drew, H. R., Takano, T., Broka, C., Tanaka, S., Itakura, K. & Dickerson, R. E. (1980) *Nature (London)* **287,** 755–758.
26. Bustamante, C., Vesenka, J., Tang, C. L., Guthold, M. & Keller, R. (1992) *Biochemistry* **31,** 22–26.
27. Bustamante, C., Keller, D. & Yang, G. (1993) *Curr. Opin. Struct. Biol.* **4,** 750–760.
28. Hansma, H. G. & Pietrasanta, L. (1998) *Curr. Opin. Chem. Biol.* **2,** 579–584.
29. Kim, T.-K., Lagrange, T., Wang, Y.-H., Griffith, J. D., Reinberg, D. & Ebright, R. H. (1997) *Proc. Natl. Acad. Sci. USA* **94,** 12268–12273.
30. Forget, D., Robert, F., Grondin, G., Burton, Z. F., Greenblatt, J. & Coulombe, B. (1997) *Proc. Natl. Acad. Sci. USA* **94,** 7150–7155.
31. Dyer, M. A., Hayes, P. J. & Baron, M. H. (1998) *Mol. Cell. Biol.* **18,** 2617–2628.
32. Horton, N. C. (1998) *J. Mol. Biol.* **277,** 779–787.
33. Luger, K. & Richmond, T. J. (1998) *Curr. Opin. Struct. Biol.* **8,** 33–40.
34. Baker, R. E., Harris, K. & Zang, K. (1998) *Genetics* **149,** 73–85.
35. Meluh, P. B., Yang, P., Glowczewski, L., Koshland, D. & Smith, M. M. (1998) *Cell* **94,** 607–613.
36. Darst, S. A., Kubalek, E. W. & Kornberg, R. D. (1989) *Nature (London)* **340,** 730–732.
37. Goh, P.-Y. & Kilmartin, J. V. (1993) *J. Cell Biol.* **121,** 503–512.
38. Jiang, W., Lechner, J. & Carbon, J. (1993) *J. Cell Biol.* **121,** 513–519.
39. Jiang, W. & Carbon, J. (1993) *Cold Spring Harbor Symp. Quant. Biol.* **58,** 669–676.